TEMPERATURE FIELDS IN HEAT-PROTECTIVE MATERIALS

V. F. Zakharenkov and L. I. Shub

UDC 536.248.2

A solution of the heat transfer equation for polymer heat-protective materials is presented for the case where three characteristic zones are established. The calculation includes the variation of thermophysical characteristics as a function of temperature and porosity of the material.

In the practical use of heat-protective materials, conditions are possible where a charred layer produced by pyrolysis is maintained on the surface. Relative to such conditions, we consider the following problem on the dispersal of heat in materials based on unfilled, hardened polyester, epoxy, and phenolic resins.

An infinite, thermally insulated polymer slab of thickness δ at an initial temperature $T = T_0 = \text{const}$ is subjected to convective heating on one side by a gas flow, the temperature of which varies with time in the following way,

$$\text{for} \quad 0 < t < t_1 \quad T_\infty = a_1 t;$$

$$\text{for} \quad t_1 < t < t_2 \quad T_\infty = a_2 t^2 + b_2 t + c_2;$$

$$\text{for} \quad t > t_2 \quad T_\infty = a_3 = \text{const},$$

and the coefficient of heat transfer is a constant. Through the action of the high temperature of the gas, thermal decomposition of the material occurs accompanied by thermal effects and the injection of decomposition products into the external flow. In these circumstances, the thermophysical characteristics of the material change. The temperature distribution over the thickness of the slab is required.

In the general case, the problem formulated can be represented as the dissipation of heat in a three-layered body represented by the system charred layer (CL)–pyrolysis zone (PZ)–undecomposed material (UM).

The first layer (CL) is a porous coke residue through which the pyrolysis products diffuse into the external gas flow. In this layer, the coking process is complete ($\Gamma = \Gamma_0$). The porosity and density of the

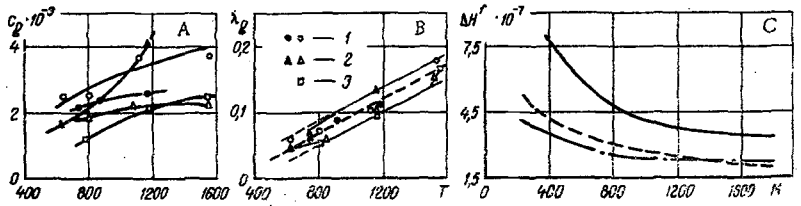

Fig. 1. Pyrolysis characteristics: a, b) respectively the dependence of heat capacity (J/kg·deg) and thermal conductivity (W/m·deg) of pyrolysis products on temperature, °K, (1-3) (open symbols) from data in [3, 6], 1-2 (solid symbols) from data in [4, 5]); c) heat of polymer formation (J/kg) as a function of molecular weight (solid curve, polyester coating; dashed curve, epoxy coating; dot-dashed curve, polyester coating).

Mechanical Institute, Leningrad. Translated from Inzhenerno-Fizicheskii Zhurnal, Vol. 25, No. 5, pp. 827-836, November, 1973. Original article submitted November 24, 1972.

material are constant over the thickness and the thermal conductivity, heat capacity, and thermal diffusivity depend only on temperature. The coefficient for heat transfer between the coke and the diffusing gas is assumed infinitely large. It is further assumed the process is not accompanied by mechanical or chemical erosion.

The second layer (PZ) is characterized by thermal decomposition of the material which occurs throughout the entire volume. Density, thermal conductivity, heat capacity, and heat of pyrolysis depend on temperature and porosity (degree of gasification of the material) and vary from the values at the CL–PZ boundary to the values at the PZ – UM boundary.

The third layer (UM) is characterized by the fact that the laws of heat dissipation here are similar to the laws for intact solids. In this layer the porosity is equal to its initial value or is zero; the density of the material is constant, and the thermal conductivity, heat capacity, and thermal diffusivity are only functions of temperature.

In proportion to the heating in the material, all three types of zones are established and they gradually transform from one to the other.

Heat transfer then reduces to a solution of the equation

$$c(T)\rho(T)\frac{\partial T}{\partial t}-\frac{\partial}{\partial y}\left[\lambda(T)\frac{\partial T}{\partial y}\right]=A\frac{\partial T}{\partial y}+B \tag{1}$$

under the conditions

$$T(0,\ y)=T_0=\text{const},\ \Gamma_{PZ}=0,\ \dot{m}_g=0,\ \xi=\zeta=0; \tag{2}$$

$$\lambda(T)\left.\frac{\partial T}{\partial y}\right|_{y=0}=\alpha[T_\omega-T_\infty(t)];\quad \alpha=\alpha^0\left(1-\eta\frac{\dot{m}_g^*}{\alpha^0/c_p}\right); \tag{3}$$

$$\lambda(T)\left.\frac{\partial T}{\partial y}\right|_{y=\delta}=0. \tag{4}$$

The quantities B and A, which characterize the volume heat sources during decomposition and heating of pyrolysis products, are calculated from

$$\text{for}\quad T>T_\xi,\quad 0<\Gamma_{PZ}<\Gamma_0$$

$$B=r(T,\ \Gamma_{PZ})\dot{m}_g; \tag{5}$$

$$A=\dot{m}_g^*(T,\ \Gamma_{PZ})c_g; \tag{6}$$

$$\text{for}\quad T<T_\xi\quad \Gamma_{PZ}=0,\quad A=B=0. \tag{7}$$

Thermophysical characteristics are determined from existing published data and through specially performed experiments and calculations.

Layer of Undecomposed Material. The studies of V. S. Bil' and N. D. Avtokratova [1] show that for the majority of polymers the variation of thermal conductivity and thermal diffusivity is of a linear nature.

$$\left.\begin{aligned}\lambda_{UM}&=a_4+b_4T\\ a_{UM}&=a_5-b_5T\end{aligned}\right\} \tag{8}$$

Charred Layer. The density of the charred layer, under the condition the coke residue is distributed uniformly over the entire layer and the volume of the material is unchanged during coking, is given by

$$\rho_{CL}=\rho_K(1-\varepsilon_{CL});\quad \varepsilon_{CL}=1-\frac{\rho_{UM}}{\rho_K}K. \tag{9}$$

Assuming the contribution of the coke and the gaseous pyrolysis products to thermal conductivity and heat capacity is proportional to their volume content, we find

$$\left.\begin{aligned}\lambda_{CL}&=\lambda_K(1-\varepsilon_{CL})+\lambda_g\varepsilon_{CL}\\ c_{CL}&=c_K(1-\varepsilon_{CL})+c_g\varepsilon_{CL}\end{aligned}\right\} \tag{10}$$

The thermal conductivity and heat capacity of monolithic coke was determined from the data in [2] in accordance with the following approximate relations:

for $300 \le T \le 1000°C$

$$c_K=3.10\cdot10^{-7}T^2+8.15\cdot10^{-4}T+1.02; \tag{11}$$

TABLE 1

Coating	Density, kg/m³	Temperature for initiation of decomposition, °K	Value of Arrhenius constants at T, °K											
			443–493			493–638			638–843			over 843		
			$E\cdot10^{-5}$, J/mole	n	k_{g_0}, sec^{-1}	$E\cdot10^{-5}$, J/mole	n	k_{g_0}, sec^{-1}	$E\cdot10^{-5}$, J/mole	n	k_{g_0}, sec^{-1}	$E\cdot10^{-5}$, J/mole	n	k_{g_0}, sec^{-1}
PN-1	1210	443	0,354	1	3,25	0,285	0,862	8,66	0,220	0,782	39,47	0,206	1	165
ÉD-6	1260	488	—	—	—	0,350	1	2,70	0,324	0,900	64,3	0,300	1	218
R-21	1275	588	—	—	—	1,075	1	$5\cdot10^5$	0,780	1	744	0,470	1	110

for $300 \leq T \leq 700$°C

$$\lambda_K = 1.78\cdot10^{-6}T^2 - 2.72\cdot10^{-3}T + 2.36; \tag{12}$$

and $\lambda_K = 1.3$ for $T > 700$°C.

The thermal conductivity and heat capacity for the products of pyrolysis were calculated from the equations for mixtures of gases. The composition of the gases in the pyrolysis products from epoxy, polyester, and phenolformaldehyde resins and their weight ratio in the mixture were taken from [1, 3-6]. Values of λ_{gi} and c_{gi} were determined from handbook data or from the Misnar relations [7]. Calculated results for λ_g and c_g are shown in Fig. 1. Analysis indicates that the thermal conductivity and heat capacity of gaseous pyrolysis products in the temperature range 300-1200°C can be represented as functions of temperature in the following way:

$$\lambda_g = 1.33\cdot10^{-4}T - 0.03, \tag{13}$$

$$c_g = a_6T^2 - b_6T - c_6. \tag{14}$$

Pyrolysis Zone. The thermal conductivity and heat capacity of the pyrolysis zone, in the case of linear dependence on porosity, are calculated from

$$\lambda_{PZ} = \lambda_{UM}(T_\xi)\frac{\rho_{PZ}-\rho_{CL}}{\rho_{UM}-\rho_{CL}} + \lambda_{CL}(T_\xi)\frac{\rho_{UM}-\rho_{PZ}}{\rho_{UM}-\rho_{CL}},$$
$$c_{PZ} = c_{PZ}(T_\xi)\frac{\rho_{PZ}-\rho_{CL}}{\rho_{UM}-\rho_{CL}} + c_{CL}(T_\xi)\frac{\rho_{UM}-\rho_{PZ}}{\rho_{UM}-\rho_{CL}}. \tag{15}$$

The density of the material in the pyrolysis zone as a function of temperature and time of heating varies in accordance with the Arrhenius law [8]

$$\frac{d\rho_{PZ}}{dt} = K_g\rho_{UM}\left(\frac{\rho_{PZ}-\rho_{CL}}{\rho_{UM}}\right)^n. \tag{16}$$

Integrating Eq. (16), we find:

for $n = 1$

$$\rho_{PZ} = \rho_{CL} + (\rho_{UM}-\rho_{CL})\,e^{-\int_{t_0}^{t} K_g d\tau}, \tag{17}$$

for $n \neq 1$,

$$\rho_{CL} = \rho_{CL} + \left[(\rho_{UM}-\rho_{CL})^{1-n} - \rho_{UM}^{1-n}(1-n)\int_{t_0}^{t} K_g d\tau\right]^{\frac{1}{1-n}}. \tag{18}$$

The mass rate of gas formation per unit area of the polymer, on the basis of mass balance, is defined as (we neglect the mass of gas in the pores of the CL and PZ)

$$\dot{m}_g^* = \int_{\xi}^{\zeta} K_g\rho_{UM}(\Gamma_0 - \Gamma_{PZ})^n\,dy. \tag{19}$$

In Eqs. (16)-(19), the coefficient for the rate of gas formation is given by

$$K_g = K_{g0}e^{\int_{T_\xi}^{T_\zeta}\frac{E(T)}{RT^2}dT} \tag{20}$$

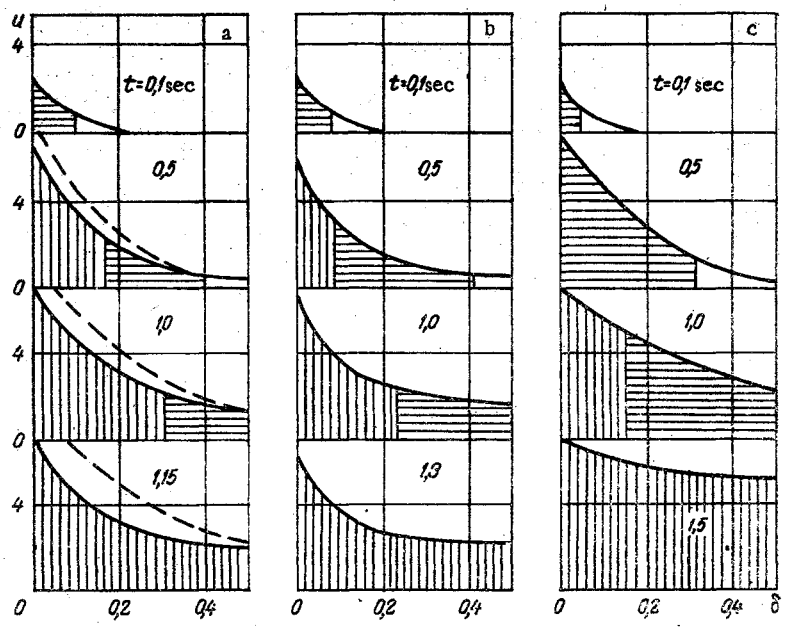

Fig. 2. Temperature field ($u = (T - T_0)/T_0$) over coating thickness δ (mm) at various times: a) polyester coating PN-1, b) epoxy coating ÉD-6, c) phenolic coating R-21; vertically hatched region is charred layer, horizontally hatched region is pyrolysis zone, and unhatched region is undecomposed material; dashed curve is temperature profile for constant thermophysical properties.

Values of the Arrhenius constants E, K_{g0} and n for each type of heat-protective material were determined experimentally. For this purpose, polymer samples were annealed in an SUOL 0.15.0.6/12M electric muffle microanalysis furnace at a constant temperature of the heated surface. Loss of polymer weight was recorded for various annealing temperatures and times, and curves $\Gamma = f(T, t)$ were constructed. To analyze the resultant experimental data, Eq. (19) was used in which the integral was calculated from the mean value

$$\dot{m}^*_{gs} = K_{ms}(\Gamma_0 - \Gamma_s)^{n_s} e^{-E_s/RT_s}, \tag{21}$$

where $K_{ms} = \Gamma_s m_0 K_{CLs}/F_t K_{gs}$. To calculate Γ_s, we used the equation [9]

$$\Gamma_s = K_{gs}(\Gamma_0 - \Gamma_s)^{n_s}, \tag{22}$$

where the subscript s indicates the value of a parameter at the average temperature in the pyrolysis zone.

In accordance with Eqs. (21) and (22) and also the resultant experimental curves $\Gamma_s = f(T_s, t)$, the reaction order, the nominal activation energy for thermo-oxidative destruction, and the coefficient for the rate of gas formation were determined from:

$$n_s = \left| \frac{d \ln \dot{\Gamma}_s}{d \ln (\Gamma_0 - \Gamma_s)} \right|; \quad E_s = R \cdot \frac{d \ln K_{gs}}{d (1/T_s)};$$

$$n = 1: K_{gs} = 1/t \cdot \ln \frac{\Gamma_0}{\Gamma_0 - \Gamma_s}; \quad n \neq 1: K_{gs} = \frac{\Gamma_0^{1-n_s} - (\Gamma_0 - \Gamma_s)^{1-n_s}}{(1-n_s)t}; \tag{23}$$

$$K_{gCL} = \frac{K_{gs}}{e^{-E_s/RT_s}}.$$

We then determined the heat of pyrolysis, which for a high molecular-weight chemical compound is equal to the difference between its heat of formation and the heats of formation of the solid and gaseous phases, i.e.,

$$r = -\Delta H_0^f + \left[\left(\sum_i \Delta H_{f_i}^0\right)\right] \Gamma_{PZ} + \Delta H_K^f (1 - \Gamma_{PZ}). \tag{24}$$

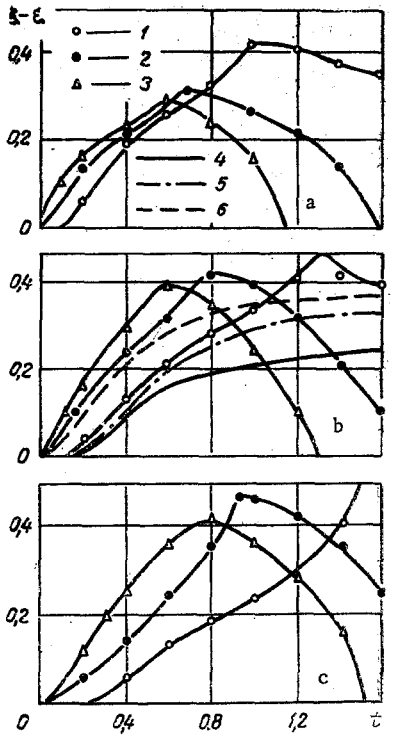

Fig. 3

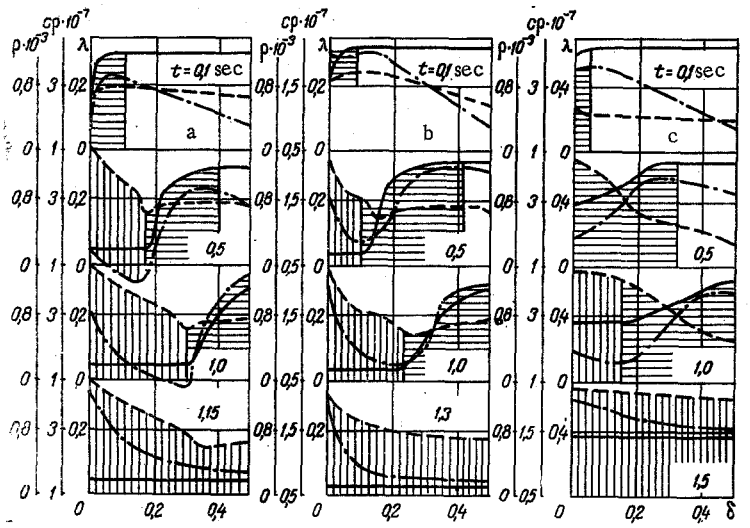

Fig. 4

Fig. 3. Variation of pyrolysis zone thickness $\xi-\zeta$ (mm) with time (sec); a) PN-1; b) ÉD-6; c) R-21; 1) $\alpha = 400$, $\delta = 0.5$ mm; 2) 2000 and 0.5 mm; 3) 10,000 and 0.5 mm; 4) 400 and 2 mm; 5) 400 and 1 mm; 6) 2000 and 2 mm.

Fig. 4. Variation of thermophysical characteristics over coating thickness at various times: a) PN-1 polyester coating; b) ÉD-6 epoxy coating; c) R-21 phenolic coating. Hatched areas correspond to those in Fig. 2. Solid curve is ρ, dot-dashed curve is $c\rho$, and dashed curve is λ; ρ in kg/m^3, $c\rho$ in J/m^3·deg, and λ in W/m·deg.

The heat of formation of the coke residue ΔH_K^f as a function of temperature was taken from [5]. The polymer heat of formation ΔH_0^f was calculated analytically. In this case, we used the recommendation of [10] according to which the heat of formation of a complex chemical compound of the type ABCD can be determined from the energies of bonds of the i-th type and the heats of formation of the gas atoms produced by complete decomposition of the compound, i.e.,

$$\Delta H_0^f = -\sum_i \nu_i h_i + \sum_j \Delta H_{faj}^0, \tag{25}$$

where $\sum_j \Delta H_{faj}^0$ is the sum of the heats of formation of the gas atoms; ν_i is the number of bonds of the i-th type; h_i is the bond energy for the i-th type. Data on bond energies needed for the calculations was taken from [11-13]. Calculated results for the heats of formation are given in Fig. 1 for the polymers considered.

The heat of formation for the gaseous mixture of pyrolysis products, $\Sigma\Delta H_{f_i}^0$, was determined from the constitution of the gaseous decomposition products and the heats of formation of the components making up the gas mixture. In this case, values of $\Delta H_{f_i}^0$ were taken either from handbooks or were calculated by the group equation method [13].

Because the value of T_s is experimentally undeterminable, the calculation of n_s, E_s, and K_{g0s} was carried out by means of successive approximation. In the zeroth approximation, the value of the temperature at the surface of the sample, T_ω, was taken as the value of T_s. Values of the Arrhenius constants obtained from Eqs. (23) for the zeroth approximation were then used for calculation of the temperature profile in the sample by solution of Eq. (1) under the conditions (2) and a boundary condition of the first kind at the external boundary. The calculated temperature profile in the pyrolysis zone was then averaged

over its thickness and a new value T_{s_1} determined which was then used for a determination of the constants n_{s_1}, E_{s_1}, and K_{gCL_1} in a first approximation from the same equations. A satisfactory accuracy was achieved for the calculations in 4-6 approximations. A check on the convergence of the method of successive approximations was realized through the time for complete decomposition of the sample. Resultant values of the kinetic constants averaged for four temperature ranges are given in Table 1.

Thus all the data required for the solution of the system (1)-(3) was obtained.

Solution of the heating problem in a heat-protective coating and analysis of the experiment were done on a computer. For this purpose, an implicit difference approximation scheme was used for Eqs. (1), (3), and (4). The approximating equations and recursion relations take the form:

$$c(U_i)\frac{U_i^l - U_i^{l-1}}{\tau} = \frac{\lambda(U_{i+1/2})(U_{i+1}^l - U_i^l) - \lambda(U_{i-1/2})(U_i^l - U_{i-1}^l)}{h^2}$$

$$+ \left\{\frac{1}{2}\left[A(U_{i+1/2})\frac{U_{i+1}^l - U_i^l}{h} + A(U_{i-1/2})\frac{U_i^l - U_i^{l-1}}{h}\right] + B(U_i)\right\}E(U_i - U_\xi) \qquad (26)$$

$$(i = -1,\ 0,\ 1,\ \ldots,\ N);$$

$$x_0 = -\frac{\alpha h + \lambda(U_0) + \lambda(U_{-1})}{\alpha h - \lambda(U_0) - \lambda(U_{-1})};\quad y_0 = \frac{2\alpha U_\infty h}{\alpha h - \lambda(U_0) - \lambda(U_{-1})};$$

$$x_{i+1} = \{\lambda(U_{i+1/2}) + 1/2hA(U_{i+1/2})E(U_i - U_\xi)\}\{\lambda(U_{i+1/2}) + \lambda(U_{i-1/2}) + 1/2h[A(U_{i+1/2}) - A(U_{i-1/2})]E(U_i - U_\xi)$$

$$+ c(U_i)\frac{h^2}{\tau} - [\lambda(U_{i-1/2}) - 1/2hA(U_{i-1/2})E(U_i - U_\xi)]x_i\}^{-1};$$

$$y_{i+1} = \left\{h^2B(U_i)E(U_i - U_\xi) + c(U_i)\frac{h^2}{\tau}U_i^{l-1} + [\lambda(U_{i-1/2}) - A(U_{i-1/2})E(U_i - U_\xi)]y_i\right\}\{\lambda(U_{i+1/2}) + 1/2hA(U_{i+1/2})E(U_i - U_\xi)\}^{-1}x_i$$

$$(i = 0,\ 1,\ \ldots,\ N-1);$$

$$U_N^l = \frac{y_N}{1 - x_N};\quad U_i^l = x_{i+1}U_{i+1}^l + y_{i+1}\quad (i = N-1,\ \ldots,\ -1),$$

where

$$E(U_i - U_\xi) = \begin{cases} 0 & \text{for } U_i < U_\xi, \\ 1 & \text{for } U_i \geqslant U_\xi; \end{cases}$$

$$h = \frac{\delta}{N},\quad U = \frac{T - T_0}{T_0}.$$

The strong dependence of thermophysical characteristics on temperature imposes a limitation on the choice of τ ($\tau < 0.01$ sec). This makes it possible to linearize Eq. (26) and to calculate the variable coefficients from the preceding time step.

The calculations were performed for a broad range of the heat-carrier coefficient α^0 (from 400 to 10,000 W/m^2·deg) and of the heat-protective material thickness (from 0.5 to 2 mm). Specific results of the calculations are shown in Figs. 2-5.

Figure 2 shows curves for the temperature over the thickness of the material at various times for polyester, epoxy, and phenolic coatings. It is clear that the chemical nature of the material, its thermophysical characteristics, thermal stability, and capacity for gas formation play an important role in the formation of the temperature field. In materials with lower coking numbers and coefficients of thermal conductivity (polyester and epoxy coatings), the temperature profile is steeper. However, despite less intense heating, the effectiveness of such coatings is less than that for phenolics because of low thermal stability.

The curves shown in Fig. 3 characterize the rate of increase in PZ thickness with time. It is clear the pyrolysis zone has a tendency to increase with an increase in the heat-transfer coefficient and a decrease in the coating thickness. The decrease in PZ thickness for large heat-transfer coefficients is associated with the emergence of the coordinate ξ at the opposite face of the coating. An intense rise in PZ thickness is observed when the pyrolysis zone is located near the boundary of the coating. Within the material, the CL–PZ and PZ–UM boundaries move at approximately the same velocity. In this case, the thickness of the PZ is comparable to the thicknesses of the CL and UM, which points to the inadmissibility in the calculations of a reduction of the PZ at the pyrolysis front.

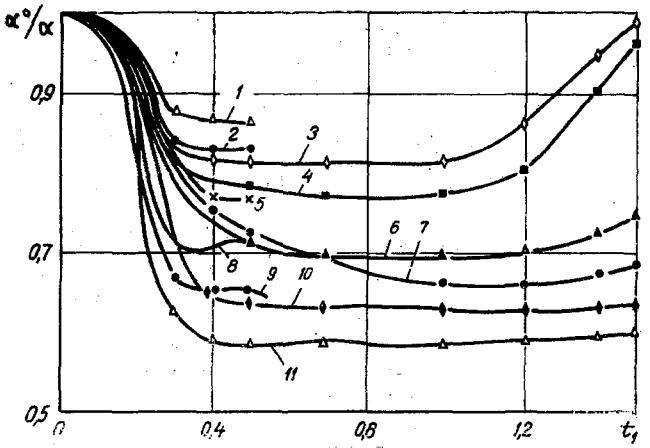

Fig. 5. Effect of pyrolysis-product injection on heat-transfer coefficient: 1, 2, 3) $\alpha = 1000$, 3000, and 5000, $\delta = 0.5$ mm; 4-7) $\alpha = 500$, 1000, 3000, and 5000, $\delta = 1$ mm; 8-11) $\alpha = 500$, 1000, 3000, and 5000, $\delta = 2$ mm; t in sec, α and α° in $W/m^2 \cdot deg$.

Variation of the thermophysical characteristics of the materials over the thickness of the coating is shown in Fig. 4. An analysis of the curves indicates that the thermophysical characteristics in the pyrolysis zone and the charred layer vary considerably with the variation being nonmonotonic and depending strongly on the current decomposition parameters.

Injection of pyrolysis products into the external flow leads to a significant reduction in the coefficient of heat transfer (Fig. 5). For example, the reduction in α° reaches 13-42% for a polyester coating.

To compare the results with calculations for constant thermophysical characteristics, a special study was made which showed the failure to allow for their variability leads to considerable error. The error in calculation of the temperature with constant values for λ, c, a, and ρ and without including injection ($\dot{m}_g^* = 0$) and the heat of pyrolysis ($r = 0$) is 60-70%. Furthermore, merely the assumption $r = 0$ leads to an error of 6-8% in temperature values and to an increase in the charring rate up to 30%.

NOTATION

t	is the time;
y	is the current coordinate;
ξ, ζ	are the boundaries of charred layer and region of pyrolysis, respectively;
T	is the temperature;
λ	is the thermal conductivity;
c	is the heat capacity;
a	is the thermal diffusivity;
Γ	is the relative fraction of material converted into gas;
m	is the volume rate of gas generation;
$\dot{m}^*$	is the surface rate of gas generation;
ρ	is the density;
r	is the heat of pyrolysis;
k_g	is the coefficient of gas generation rate;
ε	is the porosity;
n	is the reaction order;
E	is the activation energy;
R	is the gas constant;
k_{g_0}	is the pre-exponent;
ΔH	is the heat of generation;
a_i, b_i, c_i	are the constants;
η	is the coefficient allowing for the nature of gas flow around a polymer plate: for laminar boundary layer $\eta = 0.6$-0.8; for turbulent boundary layer $\eta = 0.4$-0.5;

u is the dimensionless temperature;
h is the coordinate step;
τ is the time step.

Subscripts

CL is the charred layer;
PZ is the pyrolysis zone;
UM is the undecomposed material;
∞ is the external medium;
g is the gas of pyrolysis;
0 is the limit value;
K is the coke.

LITERATURE CITED

1. V. S. Bil' and N. D. Avtokratova, Plast. Mass., No. 10 (1965).
2. Yu. A. Dushin, Performance of Heat-Protective Materials in Hot Gases [in Russian], Khimiya, Leningrad (1968).
3. S. L. Madorskii, Thermal Decomposition of Organic Polymers [in Russian], Mir, Moscow (1967).
4. M. B. Neiman, B. M. Kovarskaya, et al., Plast. Mass., No. 7 (1960).
5. Ladaki, Hamilton, and Coates, Raketnaya Tekhnika i Kosmonavtika [Russian translation], No. 10 (1966).
6. Structural Properties of Plastics (Physicochemical Bases for Application) [in Russian], Khimiya, Moscow (1967).
7. A. Misnar, Thermal Conductivity of Solids, Liquids, Gases, and Mixtures [in Russian], Mir, Moscow (1968).
8. Skala and Gilbert, Raketnaya Tekhnika, No. 6 (1962).
9. Handbook of Chemistry [in Russian], Vol. 6, Khimiya, Moscow (1967).
10. V. M. Tatevskii, Chemical Structure of Hydrocarbons and Their Physicochemical Properties [in Russian], MGU (1953).
11. L. Pauling, Nature of the Chemical Bond [Russian translation], Goskhimizdat, Moscow (1947).
12. A. A. Tager, Physical Chemistry of Polymers [in Russian], Khimiya, Moscow (1968).
13. V. A. Kireev, Practical Calculations in the Thermodynamics of Chemical Reactions [in Russian], Khimiya, Moscow (1970).